Picosecond Pump-Probe Spectroscopy of the Mott-insulating *1T*-$TaS_{1.5}Se_{0.5}$ for the Study of Material Relaxation Dynamics

Rose Albu Mustaf[1]*
[1] *Department of Physics and Astronomy, University of California, Davis, California 95616, USA*

(Dated: August 16, 2022)

Mott Insulators are materials that, according to conventional band theories, are expected to behave as conductors, but instead show insulating properties due to strong repulsion forces between their electrons. Tantalum sulfide is a transition metal dichalcogenide (TMD) and a common Mott insulator that is used in the manufacture of memory devices. The doping of tantalum sulfide with selenium causes a shift in phase transition temperature [1] and changes its conducting properties at different selenium contents and temperatures. In our research, we study the reflectivity of a 2x2 mm *1T*-$TaS_{1.5}Se_{0.5}$ sample using pump-probe picosecond spectroscopy. The purpose of the experiment is to pulse a laser beam at a particular wavelength, called the 'pump', in order to perturb our material, just picoseconds before another broad spectrum laser beam, called the 'probe' is pulsed on the sample. The probe beam is then analyzed using computer software to obtain the reflectivity spectrum of the sample in its excited state across different temperatures. This allows us to gain further insight into any hysteretic behavior the material shows, and use it to study its relaxation dynamics as well as the dynamics of its correlated electrons.

I. INTRODUCTION

Mott insulators emerge when the Coulomb interaction, which is the repulsion force between the electrons, exceeds the bandwidth in partially-filled band systems that are represented by the Hubbard model. The Hubbard model is the basic model that describes interacting electrons systems in materials and is especially useful in understanding strongly correlated electron systems [2]. Extensive research has been conducted on *1T*-$TaS_{1.5}Se_{0.5}$ and its phases, with great emphasis on its Mott-insulating phase transition.

A. Crystal Structure

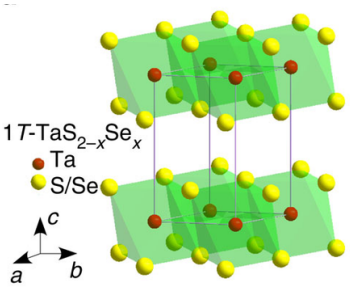

FIG. 1: Three-dimensional crystal structure of *1T*-$TaS_{2-x}Se_x$ [1]

The material consists of a central Ta atom that is octahedrally coordinated by six S or Se atoms within the P-3m1 space group. [1] One plane of the hexagonally arranged Ta atoms is centered in between two planes of the hexagonally packed S or Se atoms via weak van der Waals interactions. Figure 1 illustrates the three-dimensional crystal structure

B. Phase Diagram

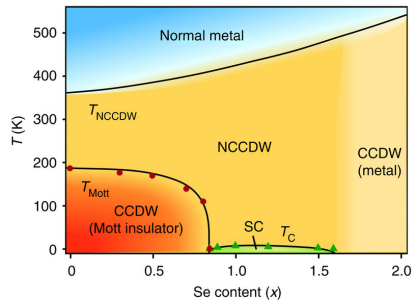

FIG. 2: Phase Diagram of *1T*-$TaS_{2-x}Se_x$ [1]

Figure 2 shows the electronic phase diagram of *1T*-$TaS_{2-x}Se_x$ as a function of the temperature T and selenium content, ranging from x=0 to x=2.0. [1] For our specific sample, with selenium content of 0.5, Mott-insluating behavior can be observed from temperatures 0 to about 180 K.

When the sample is exposed to temperatures ranging from 180 to approximately 370 K, it is in the Near-commensurate charge density wave state. Beyond 370K, the material behaves as a normal metal. This phase diagram is important in classifying and understanding the

*Electronic address: rosebertrose [at] gmail.com

behavior of the material in this experiment.

C. Pump-Probe Spectroscopy

Optical pump-probe spectroscopy is a common technique that is beneficial in understanding the non-equilibrium dynamics of materials, and can be set up to study different properties, from recombination dynamics to lattice degrees of freedom. Our specific set up aims to measure the change in reflectivity of the material, which is used as a way to monitor and study its relaxation dynamics following its photo-excitation. The change in reflectivity can reveal the processes by which photoexcited carriers return to equilibrium. [3] The experiment consists of splitting a laser beam into two beams: the 'pump', which is used to perturb and photo-excite the sample and the 'probe', which is used to monitor the reflectivity of the sample after it is perturbed. A graph of the change in reflectivity as a function of time is obtained by changing the delay time between the pump and probe pulses. This process is repeated at different temperatures ranging from 80 to 300 K, at 20 K intervals, in order to showcase the full range of its reflectivity. Other experiments have been performed to study the effect of pump fluence on transient reflectivity, and showed that the decay rate increases linearly with pump fluence. Since our experiment aims to study the temperature dependence, we maintain a constant pump fluence throughout.

II. EXPERIMENTAL SET-UP

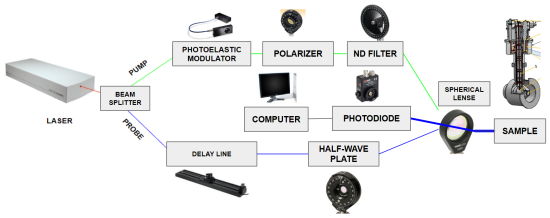

FIG. 3: Illustration of Experiment Set-Up

The experiment set up consists of an ultrafast Titanium Sapphire laser that pulses a light of 820 nm wavelength. A half-wave plate as well as a polarizer work to control the beam power of the laser. A collimator that consists of a lens pair is put into place in order to confine the beam area and change its diameter. A beamsplitter then splits the output of the laser into two beams, a 'pump' and a 'probe'. The purpose of the pump beam is to excite the tantalum sulfide sample. After splitting, the pump beam passes through a photoelastic modulator whose purpose is to modulate the intensity of the beam. An neutral density filter controls the fluence of the pump, which is the energy of the pulse per unit area.

The probe beam on the other hand, goes through a prespecified time delay through a stepper motor delay stage. The purpose of this is to change the optical path length difference of the two beams. At what is called 'time zero', the two beams hit the sample at the same time. As the delay stage moves at intervals of picoseconds, the relative timing between the pump and the probe changes. The two beams are cross-polarized, meaning that they have opposite polarization to each other. This is to prevent interference and reduce noise during data acquisition. After the two beams converge at the sample, the

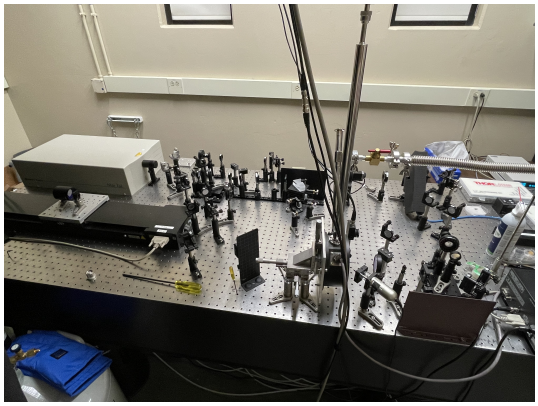

FIG. 4: Experiment Set-Up

probe then reflects off of the sample and passes through a lens that concentrates the beam. This then feeds into a photodiode whose main function is to transmit the signal into a LabJack dongle that is connected to the computer. This, along with the LabVIEW program, creates the graphs of transient reflectivity. The process of obtaining such small signals is achievable through the use of a lock-in amplifier. It is an instrument that acquires double the frequency output of the probe from the photoelastic modulator as the reference frequency, and uses that to filter the out-of-phase waves in order to measure the pump-induced changes in reflectivity.[4] Experiment

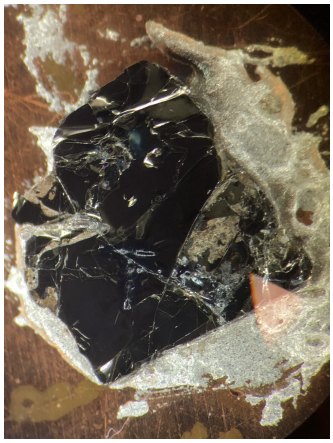

FIG. 5: $1T$-$TaS_{1.5}Se_{0.5}$ Sample Mounted on Copper Disk

controls such as delay time range, step size, and acquisition rate can be changed using a LabVIEW program. This program also allows for access to the delay stage, photodiode and lock-in amplifier outputs.

To perform the experiment at different temperatures, the sample is mounted on a copper disk using colloidal graphite and held inside a cyrostat chamber. The cryostat chamber is connected to a liquid nitrogen tank whose flow can be adjusted through a valve. A heater that is connected to the chamber works to maintain a prespecified temperature for the sample.

III. DATA

Data was collected using LabVIEW. The change in transient reflectivity (ΔR/R) was taken as a function of time in picoseconds. Two different datasets were taken, the first one includes the cooling down of the sample from 300-80 K at 20 K intervals. The second dataset includes the heating up of the sample from 80-300 K at 20 K intervals.

15 traces were taken at each temperature, and later averaged and plotted as a function of time on the figures below.

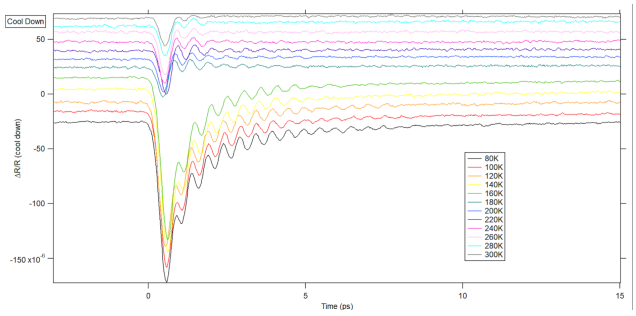

FIG. 6: Change in Reflectivity During Cool Down

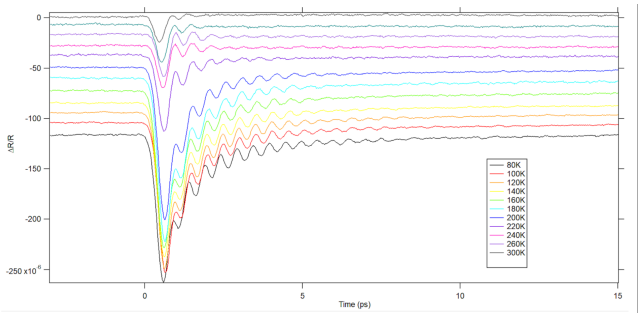

FIG. 7: Change in Reflectivity During Heat Up

IV. RESULTS AND DISCUSSION

Time zero is defined as the time the pump and probe hit the sample simultaneously. Time zero in our data can be seen very clearly from the peak directly prior to the downtrend. The decrease in reflectivity embodies the absorption of light into the sample. This is the process of excitation of the sample. Following excitation, we can see an upward oscillating trend in reflectivity back to equilibrium. The sinusoidal oscillations in the reflectivity signal is a result of coherent phonon dynamics. Generally speaking, changes in the transient reflectivity can occur for a variety of reasons, which include (1) scattering of carriers at the surface to different bands with different masses; (2) recombination of photoexcited carriers (either through surface defects or band to band transitions); and (3) diffusion of carriers away from the surface. [5] The oscillations we see in our data are specifically due to the generation of longitudinal acoustic phonons, which are strain wave packets propagating through the material as a result of the excitation from the pump beam.

As seen from the graphs, there are differences in the change in reflectivity over time as the temperature is varied both in the heat up and cooldown of the sample. In the cooldown, we see more sinusoidal oscillations in reflectivity from the relaxation of the sample. At the 180 K trace, the amplitude of the trough significantly decreases, and seems to follow the same pattern until reaching 80 K. This change in amplitude can be explained through comparison with the phase diagram of the material. We can see that our material transitions from the Mott insulating phase to the near-commensurate charge density wave state at approximately 180K during the cooldown. It is possible that the ability of the near-commensurate CDW state to carry electric current contributes to the lower amplitude of its excitation. The more frequent oscillations in the signal at lower temperatures is due to the damping of the phonon modes, which allows the probe beam to penetrate deeper into the sample and detect the coherent phonons as propagating strain pulses in the structure. [5] In the heat up, we observe a similar trend that begins at 220 K where the amplitude decreases above that temperature. We also observe more frequent oscillations at the lower temperatures.

For data analysis, we fit the decaying oscillatory wave with a single exponential function and obtained the value of the time constant for each temperature for both the cool down and heat up. We graphed the time constant as a function of temperature and obtained a hysteresis loop. Figure 8 shows the time constant hysteretic behavior.

We then obtained the energy of oscillation for each trace. This was done by multiplying the frequency obtained from a Fast Fourier Transform on the oscillatory decay, then multiplying it by the Planck constant.

$$E = hf \tag{1}$$

The energies of oscillation for the heat up and cool down were graphed as a function of temperature. Figure

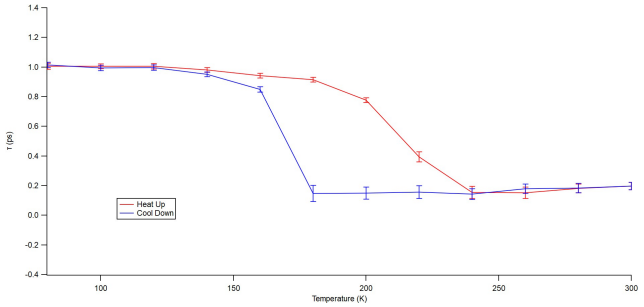

FIG. 8: Time constant (ps) vs Temperature (K) hysteresis

8 showcases the energy behavior of our material. We do not see any hysteretic trends in our energy data.

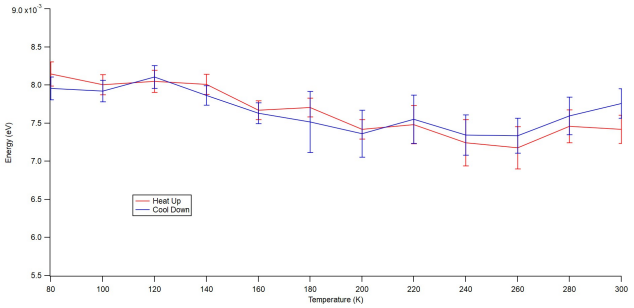

FIG. 9: Energy (eV) vs Temperature (K) behavior

The hysteretic trend for the time constant was confirmed through comparison with ARPES data. Our results be used as a reference for further experimental research. For example, our hysteresis results can work as an anchor for comparison with transport data such as resistivity and magnetization. This helps facilitate the understanding of ultrafast carrier and phonon dynamics in Mott Insulators. This way, we are able to work jointly with theory to study behavior in strongly correlated electron systems.

Future work can be done to optimize the experiment through obtaining a better cleaved sample in comparison to the one we used. A sample with a flat surface and more uniform shape provides more consistent reflectivity and less drift in the data. Another factor is the polarization of the probe beam. We later learned that the corner cube causes the beam to become elliptically polarized, and that later interferes with the pump beam as they both converge through the spherical lens before the sample. This accounts for a big part of the noise we see in our data. This can be prevented by using a quarter-wave plate, which works to circularly polarize the probe beam [6] instead of the half-wave plate in our set-up. Studying the transient reflectivity of different selenium doping in the tantalum sulfide sample is also another direction we can take with this research.

V. CONCLUSION

The purpose of this research was to obtain the reflectivity spectrum of a *1T*-$TaS_1.5Se_{0.5}$ sample as a function of temperature, and use that to explore hysteretic behaviors in the material. We performed a pump probe experiment that involved maintaining a constant fluence for the pump and probe and varying the temperature of the sample from 80-300K at 20K intervals. We showed the reflectivity of the material during both heat up and cool down, and used this to create hysteresis loops of the time constant of the decay. These hysteretic properties are beneficial in understanding material relaxation dynamics and can be used as a reference for further research involving the collapse and recovery of electronic order and other applications.

[1] R Ang, ZC Wang, CL Chen, J Tang, N Liu, Y Liu, WJ Lu, YP Sun, T Mori, and Y Ikuhara. Atomistic origin of an ordered superstructure induced superconductivity in layered chalcogenides. *Nature communications*, 6(1):1–6, 2015.

[2] Daniel P. Arovas, Erez Berg, Steven A. Kivelson, and Srinivas Raghu. The hubbard model. *Annual Review of Condensed Matter Physics*, 13(1):239–274, mar 2022.

[3] Adam L Gross, Yasen Hou, Antonio Rossi, Dong Yu, and Inna M Vishik. Nanosecond dynamics in intrinsic topological insulator bi 2- x sb x se 3 revealed by time-resolved optical reflectivity. *Physical Review B*, 103(2):L020301, 2021.

[4] Philip CD Hobbs. *Building electro-optical systems: making it all work*. John Wiley & Sons, 2022.

[5] Rathsara RHH Mudiyanselage, Brenden A Magill, John Burton, Moira Miller, Joseph Spencer, Kiara McMillan, Giti A Khodaparast, Han Byul Kang, Min Gyu Kang, Deepam Maurya, et al. Coherent acoustic phonons and ultrafast carrier dynamics in hetero-epitaxial batio 3–bifeo 3 films and nanorods. *Journal of Materials Chemistry C*, 7(45):14212–14222, 2019.

[6] Emil Wolf. *Progress in optics*, volume 47. Elsevier, 2005.